The optical properties of nickel above and below the Curie temperature

M. SHIGA† and G. P. PELLS

Solid State Division, Atomic Energy Research Establishment, Harwell, Didcot, Berks.

MS. received 29th April 1969

Abstract. The temperature dependence of the optical absorption spectrum of nickel has been measured over the wavelength range of $0 \cdot 21$–$2 \cdot 7$ μm by means of Drude's method up to 500 °K in ultra-high vacuum. The following characteristics were found: (i) a small bump near 1·4 ev which nearly disappears above the Curie temperature, whose energy is unchanged with temperature; (ii) a large absorption peak centred at about 5 ev. The peak position decreases linearly with temperature at a rate of $4 \cdot 4 \times 10^{-4}$ ev °K^{-1}. The width of this peak decreases with increasing temperature up to the Curie temperature. The change in width is interpreted in terms of exchange splitting of the bands. We assign the low energy (1·4 ev) bump to the transition between the bands near the W and K symmetry points and the main peak (~ 5 ev) to the transition from $L_{2'}$ to L_1 upper.

1. Introduction

In the preceding paper (Pells and Shiga 1969) we have shown that studies of the temperature dependence of optical absorption are very useful for analysing the optical spectrum of noble metals such as copper and gold. A similar study of nickel, which has many similarities to copper, is of particular interest since this metal is generally believed to be an itinerant ferromagnet and, therefore, it is likely that the change of band polarization with rising temperature is reflected in the optical spectrum. From an experimental point of view, fairly extensive studies have been made of the optical properties of nickel at room temperature over a wide range of photon energies (Beattie and Conn 1955, Roberts 1959, Ehrenreich *et al.* 1963). However, there have been few experiments at high temperature. Yarovaya and Timchenko (1968) reported no difference in reflectivity above and below the Curie temperature except for a very small (1%) change near 4 ev. Blodgett and Spicer (1966) also did not observe any appreciable change between room temperature and 400 °c in their photo-emission study. Considering the big change of band splitting with rising temperature, these results appear rather surprising. It seemed quite possible that a more detailed investigation might detect some systematic change in the optical spectrum of nickel.

Although studies of optical absorption may give quantitative information on band structure, there is often great difficulty in interpreting the spectrum. Conventionally it was thought that crystal momentum *k* should be conserved in inter-band optical transitions. However, on the basis of photo-emission studies, Blodgett and Spicer (1966) have argued that, in the case of nickel, the crystal momentum is not conserved at least in the high photon energy range (E > 1 ev) and have concluded that optical absorption can be understood assuming non-*k* conservation by using the optical state density curves obtained from photo-emission experiments. However, suspicion has been cast on this interpretation because new photo-emission experiments by Eastman and Krolikowski (1968) revealed that the anomalous peak 4·5 ev below E_F, which was found by Blodgett and Spicer and to which the main peak of the optical spectrum was attributed, is surface sensitive and has a much lower amplitude under clean surface conditions. On the other hand, simple reflectivity and piezo-reflectivity measurements in the low energy region (E < 2 ev) are interpreted in terms of direct transitions (*k* – conservative) (see, for example, Ehrenreich *et al.* 1963 and Hanus *et al.* 1967, 1968). So it would appear that the controversy concerning the correctness

† Now at Department of Metal Science and Technology, Kyoto University, Sakyoku, Kyoto, Japan.

of direct or non-direct transitions is still unsolved. Notwithstanding these difficulties, it was hoped that measurements of the temperature dependence of optical absorption might enable us to distinguish the contradicting mechanisms as well as to find the origin of the absorption peaks.

2. Experimental procedures

The optical constants were measured by Drude's method from $0\cdot21$ μm ($\sim6\cdot0$ ev) to $2\cdot7$ μm ($\sim0\cdot5$ ev). The details of the apparatus were reported elsewhere (Pells 1967). Measurements were made over a temperature range of 77–770 °K in a continuously pumped spectrosil chamber at a pressure of about 10^{-10} torr, except at 770 °K where the pressure rose to about 10^{-9} torr. In order to avoid interference from the light emitted by the hot specimens, phase sensitive detection techniques were used at all wavelengths.

Measurements were made on two samples prepared from completely different sources. The first sample was prepared as follows. An arc-melted ingot of Johnson Matthey's spec-pure nickel was machined into the appropriate shape ($20 \times 20 \times 5$ mm), then annealed in an evacuated silica tube at 1300 °K for two days. Mechanical polishing was carried out in the conventional way with a final polish using diamond powder of $< 1\mu$. After polishing and water washing, the sample was ultrasonically washed in absolute methyl alcohol and dried with a cold air blast. (Due to slight micro-porosity we were unable to produce a satisfactory electropolished surface.) The sample was placed in the vacuum system and rough pumped within less than half an hour of final polishing. The second sample was made from Koch-Light 99·999% pure nickel powder. It was first deoxidized in flowing hydrogen at 800 °K for four days and then argon-arc melted. Then the same treatment was given as the first sample. In this case, however, the mechanical polishing was finished with a diamond powder of 15μ. This coarse polished sample was electropolished using a nickel electropolishing solution (450 g phosphoric acid, 200 g aluminium sulphate and 15 g nickel sulphate) in the recommended condition (see Roberts 1959). A shiny surface almost free from pits was obtained. The sample was washed and dried in the same way before being placed in the vacuum system. With all samples the system was baked out at 670 °K for three days (including the raising and lowering period). The pressure was maintained at 10^{-5}–10^{-6} torr during baking.

Seib and Spicer (1968) reported that a clean nickel surface can be obtained by heating the bulk sample at 870 °K in ultra-high vacuum. In order to examine the thermal cleaning effect, measurements at several temperatures were carried out before and after reaching maximum temperature (770 °K). The sample was kept at least twelve hours at each temperature before starting a measurement. One set of measurements at each temperature took at least two days. At the highest temperature (770 °K), the sample was maintained for three days at 10^{-9} torr.

3. Results

3.1. *Thermal cleaning effect*

Figure 1 shows the optical absorption at several temperatures. These data were obtained from the second sample (electropolished) after thermal cleaning at 770 °K. At room temperature, the absorption curve shows a small bump at about $1\cdot4$ ev and a large absorption peak at about 5 ev. Hereafter, we shall refer to the former as the 'low energy' bump and the latter as the 'main peak'. Figure 2 and figure 3 show the position of maximum absorption and the width of the main peak against temperature for both electropolished and mechanically polished samples after thermal cleaning. Here the width of the main peak was defined as the distance between the points where $2nk/\lambda = 5$ μm^{-1} below the peak value. The two sets of data agree well within experimental error.

Apparent disagreements were observed between the two samples for data taken before thermal cleaning. The main features of the disagreements are:

(i) An unclean surface gives the weaker bump.

(ii) With regard to the main peak, the mechanically polished, unclean surface gives a peak position higher in energy by about $0\cdot1$ ev. For the electropolished sample, this discrepancy is smaller than for the mechanically polished one.
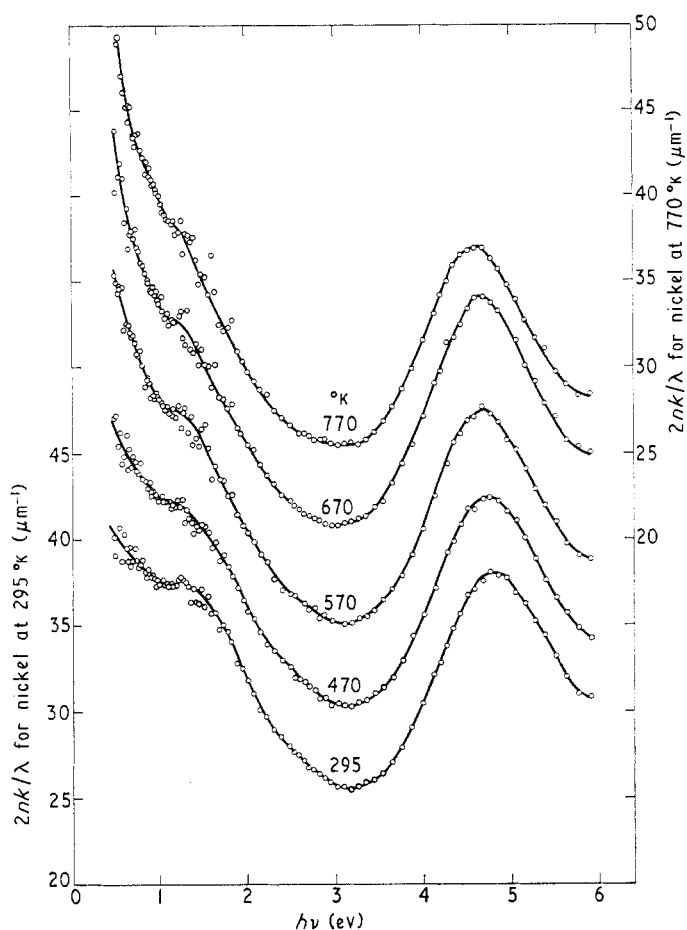
Figure 1. The optical absorption $(2nk/\lambda)$ of electropolished nickel at several temperatures. The ordinate scale is applicable only to the room temperature data. Successively higher temperatures are displaced upwards by $2nk/\lambda = 5\ \mu m^{-1}$.
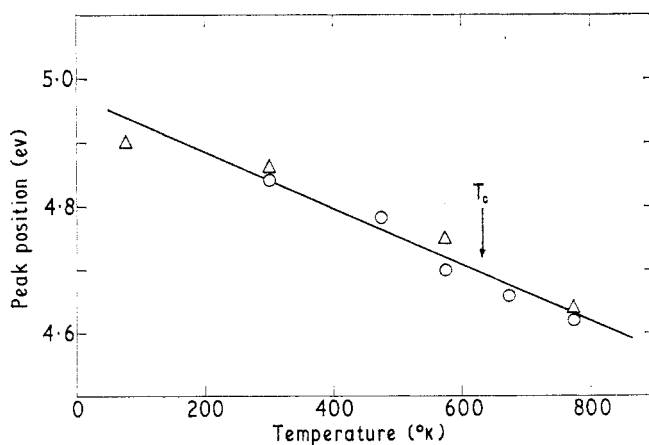

Figure 2. The energy of the main absorption peak against temperature. ○ data for electropolished sample; △ data for mechanically polished sample.

These facts suggest that the heat treatment at 770 °K in ultra-high vacuum quite effectively cleans the surface. Therefore, we give the results obtained for the electro-polished sample after thermal cleaning as a final result in figure 1.
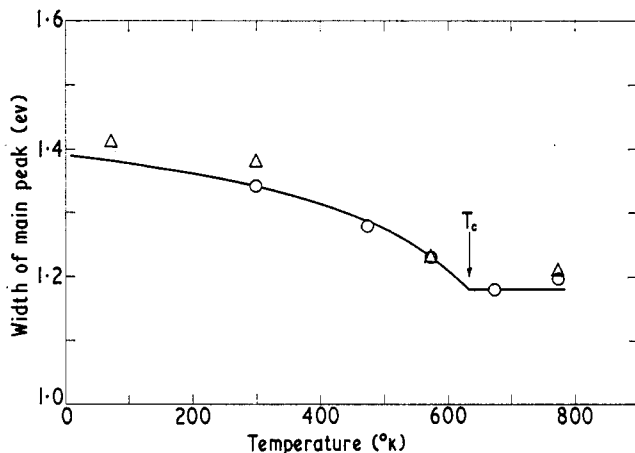

Figure 3. The width of the main peak against temperature. The width is defined as the distance between the points where $2nk/\lambda = 5 \ \mu m^{-1}$ below the peak value. ○ data for the electropolished sample, △ data for the mechanically polished sample. The full curve was calculated as described in the text.

3.2. *The spectrum at room temperature*

Comparing our results obtained at room temperature with those of Ehrenreich *et al.* (1963) we find that the general features of the spectrum are quite similar. However, a certain amount of discrepancy is observed, especially with regard to the main peak. Our peak height is almost 50% higher than theirs. In the preceding paper, we mentioned that the measurement in ultra-high vacuum gives generally higher values for $2nk/\lambda$ of noble metals. In a similar way the discrepancy from the earlier work may be attributable to the differences in surface condition.

3.3. *The effect of raising the temperature*

The significant feature in the low energy range is the decrease in the strength of the bump. Two facts should be noted. Firstly, although the bump is gradually reduced by raising the temperature and appears to nearly disappear above the Curie temperature, a trace of the bump still remains even at 770 °K. Secondly, the position of the bump, especially the edge at 1·1 ev remains unchanged at higher temperature.

With regard to the main peak, it was observed that the position of maximum absorption, and the width of the peak, change slightly with temperature. As seen from figure 2, the position moves to the lower energy side almost linearly with temperature, even above the Curie temperature.

Figure 3 shows that the width of the main peak decreases with increasing temperature. In contrast to the behaviour of the peak position however, it seems to become constant above the Curie temperature.

With regard to the strength of the absorption, no systematic change beyond the inherent error of measurements were observed.

4. Discussion

4.1. *The low energy bump*

The bump near 1·4 ev has been assigned to several interband transitions. They can be classified into two types. The first assigns it to the transition near the centre of the (111) face of the Brillouin zone (the L symmetry point). Figures 4(*a*) and 4(*b*) show examples of
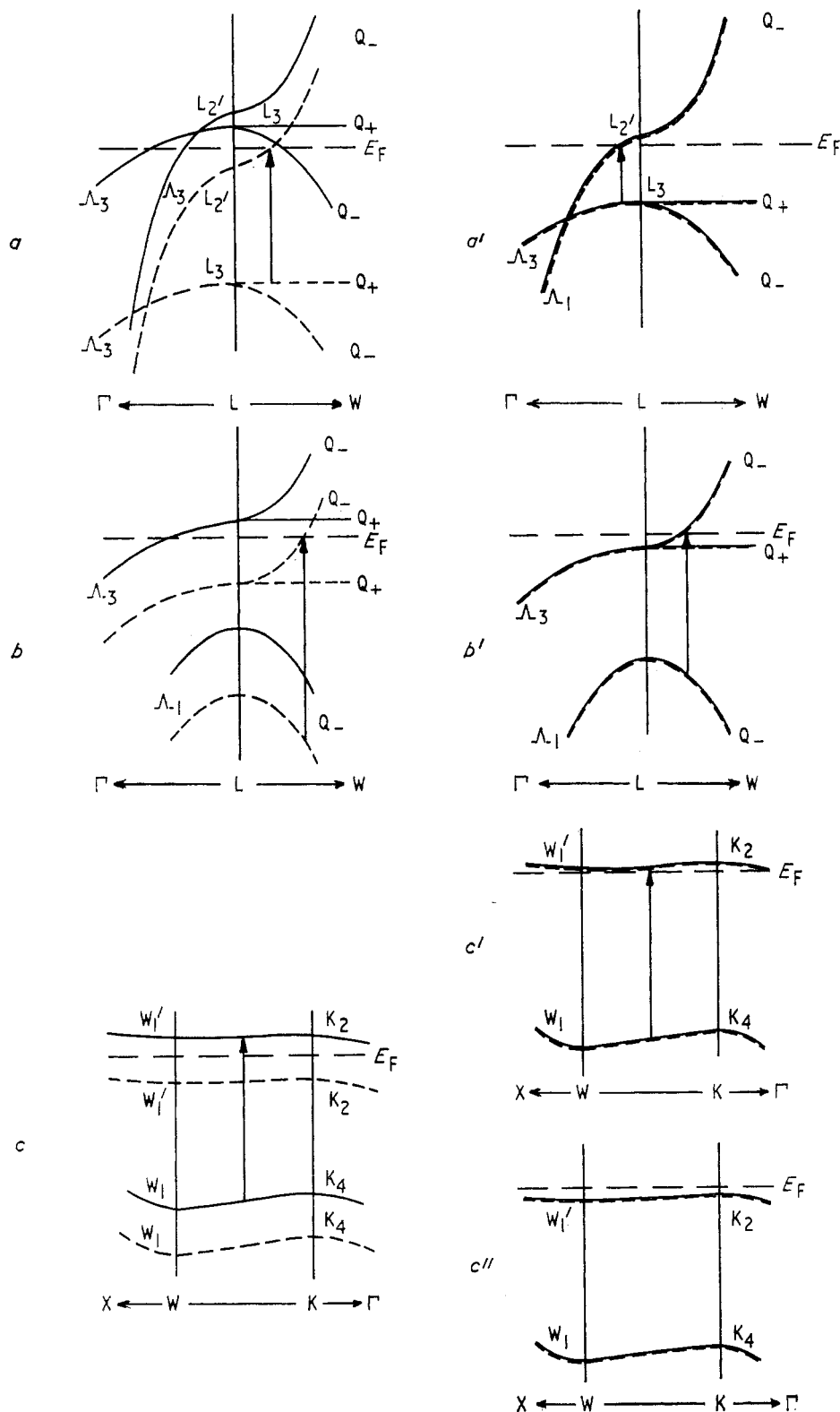
Figure 4. Possible band models to explain the low energy bump near 1·4 ev. (a) After Ehrenreich *et al.* (1963). (b) After Hanus *et al.* (1967). (c) The possible transition near the W and K points. Full curves, spin down bands; broken curves, spin up bands. (a), (b), (c), ferromagnetic state; (a′), (b′), (c′), (c″), paramagnetic state.

this kind. Let us consider the effect of raising the temperature. Figures 4(a') and 4(b') show the band structures which are expected in the paramagnetic state on the assumption that each band comes just at the centre of the ferromagnetic spin up and spin down bands. As seen from the figure, it is expected that the transition energy, especially that of the absorption edge, should change. This is not consistent with experiment.

Another model assigns the bump to the transition between bands near the W symmetry point. (Strictly speaking, the transition from W_1 to W' is not allowed just at this symmetry point, since both states have the same even parity.) Figure 4(c) shows the band structure near the W and K points and possible transitions between them. Figure 4(c') and 4(c'') show the bands in the paramagnetic state. In this case, the opposite tendency is expected with regard to the change of absorption strength depending on whether the upper band comes above or below the Fermi level. Assuming the upper band comes below the Fermi level in the paramagnetic state (figure 4(c'')), we can expect the reduction of absorption which was observed in the present study. Thermal broadening of the Fermi distribution function can explain the reason why the trace of absorption still remains above the Curie temperature, and also why the strength of the bump decreases gradually. It should be noted that this model does not cause the energy gap between the bands to change at least to a first approximation.

4.2. *The origin of the main peak*

As mentioned in § 1, the non-direct transition interpretation of Blodgett and Spicer has become suspect in the light of later photo-emission experiments. Also, it seems impossible to reproduce the observed optical spectrum by using the equation

$$nk\omega = \frac{B}{\omega} \int_{E_F}^{E_F + \hbar\omega} M^2 N_c(E) N_v(E - \hbar\omega) \, dE$$

(see Blodgett and Spicer 1966) and the new optical state density curve ($N_c(E) \cdot N_v(E)$) obtained by Eastman and Krolikowski (1968) although this simple equation might explain the large background absorption of nickel. So, we restrict further discussions to the conventional direct transition mechanism.
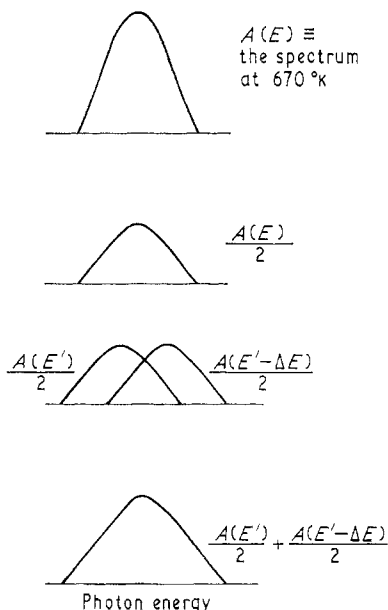

Figure 5. Schematic diagram showing how the main peak, below the Curie temperature, is constructed. ΔE is chosen to give the best fit between the calculated and observed spectra.

Before discussing the origin of the main peak, we shall show that the change of shape of the main peak can be explained as a superposition of two peaks separated by ΔE, which is proportional to spontaneous magnetization. The analytical method is schematically illustrated in figure 5. The spectrum at 670 °K is chosen as the basic unsplit spectrum rather than 770 °K as it had a slightly narrower width probably due to the longer time at high temperature. The results of the analysis are given in figure 6, where the open circles
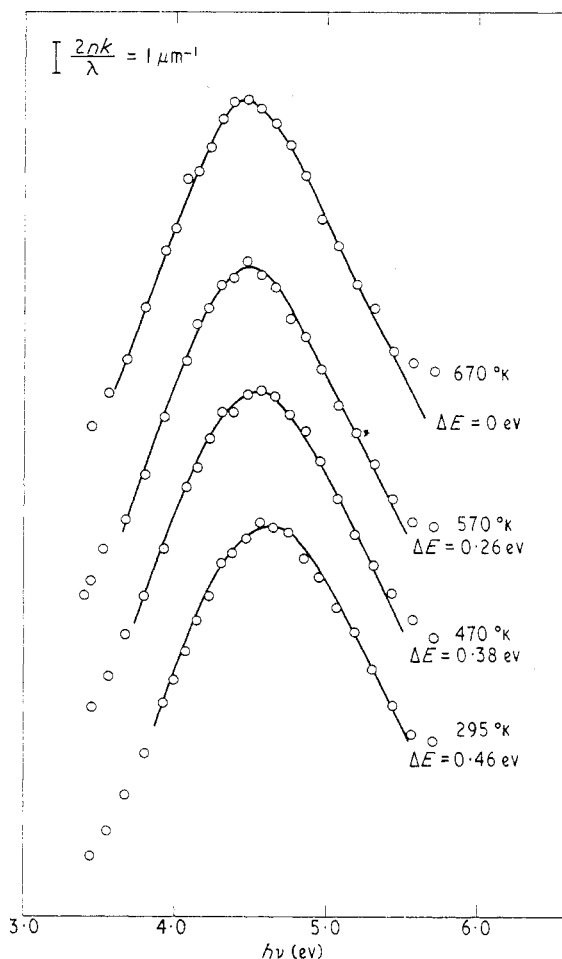

Figure 6. Comparison between the calculated and observed spectra of the main peak. Open circles, experimental points; full curve, calculated spectra.

represent the experimental data and full curves are the calculated spectra for the appropriate ΔE, which is taken so as to give the best fit with the experimental points. We obtained a very good fit as seen in the figure. The ΔE thus obtained are plotted as a function of reduced temperature (T/T_c) in figure 7. The magnetization curve reduced by the ΔE at room temperature is given in the same figure. Surprisingly good agreement was obtained between them. Conversely, assuming that ΔE is exactly proportional to the magnetization, we can estimate the width of the main peak as a function of temperature. A full curve in figure 3 shows the result of the estimation. It should be noted that this model predicts that the width should not change above the Curie temperature as observed experimentally. On the other hand, the position of the maximum absorption decreases linearly with temperature even above the Curie temperature. This suggests that the displacement of the peak is not due to the band splitting of ferromagnetism, but originates in thermal expansion in a similar way to copper.

Now let us discuss the origin of the main peak. By analogy with copper the origin of the main peak can be attributed to at least two mechanisms. One is the transition from $L_{2'}$ to upper L_1. (There are two L_1 at the L symmetry point. We describe the upper one as $L_1{}^u$ and the lower as $L_1{}^l$.) The other is the transition from near the bottom of the 3d
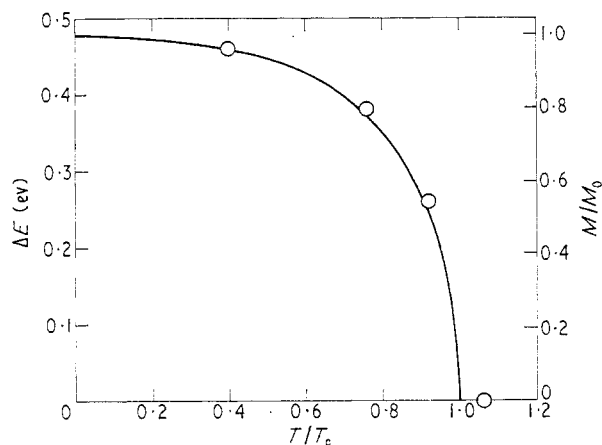

Figure 7. ΔE and the reduced spontaneous magnetization as functions of reduced temperature. The ordinate for the magnetization is chosen to coincide with ΔE at room temperature.

bands to conduction bands above the Fermi level such as $Q+$ (near $L_1{}^l$) to $Q-$ (near $L_{2'}$) and $\Delta 1$ (near X_1) to upper $\Delta 1$ (see Band scheme of Mueller and Phillips 1967). Here the position of $L_{2'}$ with respect to the Fermi level is very important for our discussions. Recent band calculations of nickel (Wakoh 1965, Connolly 1967) suggest that they are below the Fermi level for both spin directions. This conclusion is strongly supported by the de Haas–van Alphen effect (Joseph and Thorsen 1963, Tsui and Stark 1966). We shall assume that $L_{2'}(\uparrow)$ and $L_{2'}(\downarrow)$ are below the Fermi level. Figure 7 shows the band structure near L and possible transitions on which the further discussions are based. Firstly let us consider the band splitting. In the case of the first mechanism, that is $L_{2'} \rightarrow L_1{}^u$, exchange splitting of the peak can be expressed as

$$\Delta E = 0.46\,\mathrm{ev} = \Delta E(L_{2'}) - \Delta E(L_1{}^u)$$

where one can see the meaning of $\Delta E(L_{2'})$ and $\Delta E(L_1{}^u)$ in figure 8. With regard to $\Delta E(L_{2'})$, several estimates have been made. The values, which are listed by Phillips (1968), range widely between 0 and 0.7 ev. No estimates have been made for $\Delta E(L_1{}^u)$. Taking $\Delta E(L_{2'})$ as 0.4 ev one gets $\Delta E(L_1{}^u) = -0.06$ ev. Since $L_1{}^u$ has s character in contrast to the p character of $L_{2'}$, it would not be surprising that $\Delta E(L_{2'})$ and $\Delta E(L_1{}^u)$ have quite different values and even have opposite signs.

In the case of the second mechanism, that is the transition from the bottom of the 3d bands to the conduction band, the splitting of absorption edges can be expressed by

$$\Delta E = 0.46\,\mathrm{ev} = \Delta E_{3d}\,(\mathrm{bottom})$$

$$\simeq \Delta E(L_1{}^l).$$

It is possible to estimate ΔE from band calculations. According to Wakoh (1965), ΔE is estimated as 0.65 ev. Connolly's calculation (V_4) gives $\Delta E = 0.45$ ev. So we find that both mechanisms can reasonably explain the observed splitting of the peak.

With regard to the displacement of the peak position, analogy with copper suggests that the first mechanism ($L_{2'} \rightarrow L_1{}^u$) gives a larger temperature dependence than the second. It should be noted that the rate of displacement is similar to that of the main peaks of copper and gold, as shown in table 1.
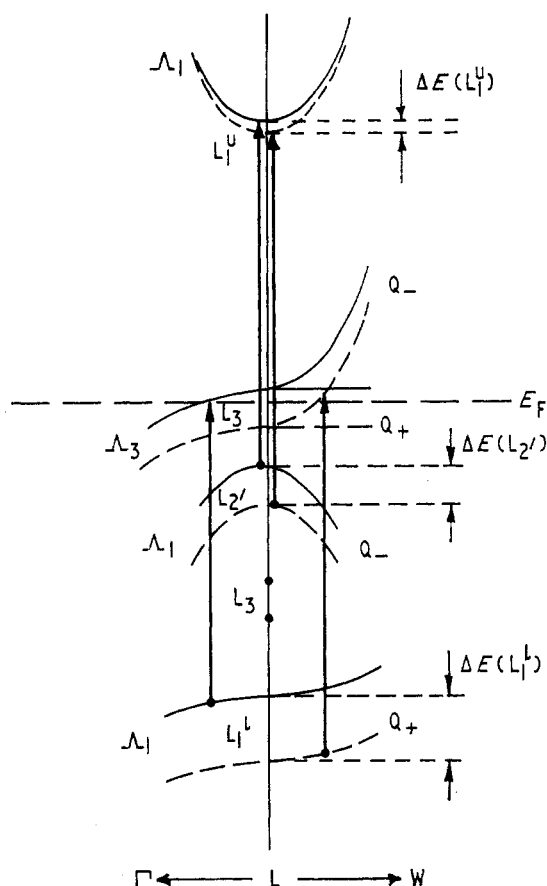
Figure 8. The band structure near the L point. Full curves are spin down bands. Broken curves are spin up bands. The definition of $\Delta E(L_1{}^u)$, $\Delta E(L_{2'})$ and $\Delta E(L_1{}^l)$ are given in this figure. The vertical arrows show the possible transitions.

Table 1. Temperature dependence of energy separation between L_2 and $L_1{}^u$

$$\frac{dE(L_{2'}-L_1{}^u)}{dT} \times 10^{-4}(\text{ev }^{\circ}\text{K}^{-1})$$

	experimental	calculated
Ni	$-4\cdot4$	—
Cu	$-6\cdot8^{a}$	$-4\cdot9^{b}$
Au	$-5\cdot2^{a}$	—

a, Obtained in the preceding paper (Pells and Shiga 1969).
b, From the band calculation as a function of lattice spacing by Davis *et al.* (1968).

It is worth while mentioning the shape of the main peak to be expected from each mechanism. The second mechanism ($L_1{}^1$, $X_1{}^1 \rightarrow E_F$) predicts the existence of an absorption edge, or in other words, an asymmetric shape for the spectrum. On the other hand a rather symmetric shape of the spectrum is expected from the first mechanism, since the contribution to the absorption can be attributed mostly to the transition between the singular points $L_{2'}$ and $L_1{}^u$.

Finally, with regard to the strength of the absorption, we concluded that both mechanisms contribute to the main peak of copper with the same order of magnitude. In the case of nickel however, we have shown that the change of the main peak with temperature is explained by a superposition of two similar peaks separated by ΔE and that the change of the peak position is simply expressed as a linear function of temperature; one can conclude that one of the mechanisms should be dominant as the origin of the main peak. Then which mechanism is more acceptable? The following facts support the first mechanism $(L_{2'} \rightarrow L_1^u)$ as the origin of the main peak of nickel. Firstly, the temperature dependence of the peak position is similar to that of the peak of gold and copper which we assign to the transition $L_{2'} \rightarrow L_1^u$. Secondly, the shape of the main peak is almost symmetric. It should be noted that the shape of the $L_{2'} \rightarrow L_1^u$ transition peak of copper which we obtained from the analysis described in the preceeding paper is quite similar to the main peak of nickel. The difference between copper and nickel can be explained as follows. Mueller and Phillips argued that the oscillator strength of the transition from L_1^1 (s–d mixed state) to $L_{2'}$ (p state) is very sensitive to the rate of s–d mixing, so it is possible that in the case of nickel this transition is greatly reduced.

Acknowledgments

Note: Values of n and k are available, on request, from the authors.

References

BEATTIE, J. R., and CONN, G. K. T., 1955, *Phil. Mag.*, **46**, 989–1001.
BLODGETT, A. J., and SPICER, W. E., 1966, *Phys. Rev.*, **146**, 390–402.
CONNOLLY, J. W. D., 1967, *Phys. Rev.*, **159**, 415–26.
DAVIS, H. L., FAULKNER, J. S., and JOY, H. W., 1968, *Phys. Rev.*, **167**, 601–7.
EASTMAN, D. E., and KROLIKOWSKI, W. F., 1968, *Phys. Rev. Lett.*, **21**, 623–7.
EHRENREICH, H., PHILIPP, H. R., and OLECHNA, D. J., 1963, *Phys. Rev.*, **131**, 2469–77.
HANUS, J., FEINLEIB, J., and SCOULER, W. J., 1967, *Phys. Rev. Lett.*, **19**, 16–20.
JOSEPH, A. S., and THORSEN, A. C., 1963, *Phys. Rev. Lett.*, **11**, 554–6.
MUELLER, F. M., and PHILLIPS, J. C., 1967, *Phys. Rev.*, **157**, 600–7.
PELLS, G. P., 1967, *J. Sci. Instrum.*, **44**, 997–1000.
PELLS, G. P., and SHIGA, M., 1969, *J. Phys. C (Solid. St. Phys.)*, [2], **2**, 1835–46.
PHILLIPS, J. C., 1968, *J. Appl. Phys.*, **39**, 755–61.
ROBERTS, S., 1959, *Phys. Rev.*, **114**, 104–15.
SEIB, D. H., and SPICER, W. E., 1968, *Phys. Rev. Lett.*, **20**, 1441–4.
TSUI, D. C., and STARK, R. W., 1966, *Phys. Rev. Lett.*, **17**, 871–7.
WAKOH, S., 1965, *J. Phys. Soc. Japan*, **20**, 1894–901.
YAROVAYA, R. G., and TIMCHENKO, L. I., 1968, *Sov. Phys.–Solid St.*, **10**, 983–4.